Electric Power Systems Research 79 (2009) 606–614

Contents lists available at ScienceDirect

Electric Power Systems Research

journal homepage: www.elsevier.com/locate/epsr

An efficient procedure to design passive *LCL*-filters for active power filters

M. Tavakoli Bina*, E. Pashajavid

Faculty of Electrical Engineering, K.N. Toosi University of Technology, Seid Khandan, P.O. Box 16315-1355, Tehran 16314, Iran

ARTICLE INFO

Article history:
Received 31 March 2008
Received in revised form 21 August 2008
Accepted 25 August 2008
Available online 16 October 2008

Keywords:
Active power filter
Passive filter design
Power system
Hysteresis

ABSTRACT

Variable high switching frequencies in grid-connected active power filters could lead to low harmonic performance and expose power systems to EMI issues too. A low-pass passive *LCL*-filter is usually used to interconnect a power electronic converter to a grid system. (This can also be done by using a passive *L*-filter.) Nevertheless, designing an *LCL*-filter is not simple because of high compensating bandwidth and variable frequency modulations involved in active filters. This paper examines various effective conditions on designing this kind of passive *LCL*-filters. Then it will propose a comprehensive design procedure in which both the outcomes of the active filter and the network obligations are taken into account. Principal advantages of this proposal are reduction of power losses of the passive filter, lowering the converter's switching ratings and the simplicity of the suggested design algorithm. A typical grid-connected shunt active filter is considered, and the needed interconnecting *LCL*-filter is designed using the proposed method. Then, the whole system is simulated with SIMULINK to verify the discussed procedure. Simulations confirm substantial reduction in power losses and converter current ratings.

1. Introduction

Active power filters are gaining more popularity due to their ability of handling higher switching frequencies by using faster power switches (e.g. IGBT) and employing digital signal processors with ultra-fast processing time. Conventionally, an inductance *L* interconnects the converter of the active filter to the grid network, thus acting like a passive low-pass filter. The bigger the inductance *L*, the higher the attenuation of high frequency components will be. Another reason for increased popularity of passive *LCL*-filters is that they show higher harmonic performances compared to a single inductance. Improper design of *LCL*-filters could lead to some inefficiency in active filters' performance [1], resonance, and instability amongst other possible consequences.

Various approaches are suggested to analyze passive *LCL*-filters for utilization as an interface between power electronic converters and grid systems [1]. However, deciding on the *LCL* parameters is not discussed there. Further, steady state and dynamic performance of passive *L*-filters are compared with those of *LCL*-filters when they interconnect power electronic converters to the power networks [2]. Also, in [3], the design of PI-controller is analyzed for the grid-connected converters, and so are the effects of the parameters of an *LCL*-filter on the performance of the controller.

A modern recursive method was suggested in [4] by trial and error method to decide on *LCL* parameters of a grid-connected voltage source inverter. But the design characteristics have no mechanism to prevent the possible increase of both power losses and the ratings of the switches. Also, selection of the initial values of the inductors is difficult at the start of the design process. Later, a method is proposed in [5] to select the initial values of inductors of the *LCL*-filter, for the purpose of simplifying the cited method in [4]. This proposal is based on using phasor relations, which is clearly not useful for active filter applications. In general, the whole method is still complex. Further, *LCL*-filters for grid-connected distributed generations are considered in [6] by focusing on the ratio of the two inductances on the two arms of the filter along with the relation of this ratio to the capacitance of the passive filter.

It should be noted, however, that the design of an *LCL*-filter for the *grid-connected active filter applications* is not reported in the literatures. Proper design of a passive *LCL*-filter for active-filtering applications is a crucial and delicate task. The reason is that control and modulation of active filter applications are different from those of voltage regulators, reactive power controllers, speed controllers of electric rotating machineries, or renewable energy applications. Since active filters are ideally designed to operate within a possible wide frequency bandwidth of the load, design and configuration of the parameters of the *LCL*-filter is a sensitive action.

This situation becomes more challenging when active filters are modulated with a typical hysteresis-like current-control technique, as shown in Fig. 1(a). The inductance and the instantaneous voltage along with the hysteresis-band determine variable duration

* Corresponding author. Tel.: +98 21 88462174x7; fax: +98 21 88462066.
E-mail address: tavakoli@kntu.ac.ir (M. Tavakoli Bina).

0378-7796/$ – see front matter © 2008 Elsevier B.V. All rights reserved.
doi:10.1016/j.epsr.2008.08.014

switching instants. Therefore, although exhibiting fast dynamic approach to the reference waveform target, a variable frequency modulator is introduced here. Moreover, due to the switch-on and switch-off transitions, high frequency spectra cause electromagnetic interference that calls for a proper electromagnetic interference (EMI) filter design. It is noticeable that these kinds of emissions can be attenuated by appropriate physical development of inductances and capacitance of the *LCL*-filter [7]. Considering Fig. 1(b), the performance goal of the passive *LCL*-filter designed for an active filter can be summarized as lowering high frequency distortions and disturbances on i_2 due to the switching as much as possible. This depends on the compensating bandwidth of the active filter and poles of the *LCL*-filter in order to avoid instability. Other problems also are taken into consideration such as power losses on stabilizing resistance, cost and ratings of the switches.

This paper contributes a comprehensive analysis of designing a passive *LCL*-filter for the shunt active filter that is modulated by using variable switching frequency techniques. Different aspects of designing an *LCL*-filter are discussed, and a design procedure is subsequently presented for passive *LCL*-filters. First, the total required inductance is decided on, such that the switching frequency remains lower than a certain upper-limit. Then, the resonance frequency is discussed wherein two design parameters have to be decided on; the inductance ratio and the capacitance of the *LCL*-filter. Then the stabilizing resistance of the passive *LCL*-filter is selected, which is worked out in accordance to the power losses of the passive filter. Proper design of these parameters is also discussed, that is crucially important for the efficiency and converter current rating. Furthermore, the insertion loss related to the EMI is analytically discussed. To verify the proposed design algorithm, a passive *LCL*-filter is designed for a typical grid-connected active power filter. It is then simulated with SIMULINK. Simulations together with the provided comparative results confirm the usefulness of the suggested procedure on lowering the power losses and current rating of the switches of the active filter.

2. Design considerations

To design a passive *LCL*-filter for active-filtering applications, the following characteristics could be taken into consideration:

- *Cost of the total inductor*: Considering Fig. 1(b), let us define two parameters (L_d and k) for the two inductances of the *LCL*-filter (L_1 and L_2) as below:

$$L_d = L_1 + L_2, \quad L_2 = kL_1 \tag{1}$$

The total inductance L_d sets an upper-limit to the switching frequency such that a bigger L_d is related to a lower switching frequency. Therefore, a minimum inductance is worked out using the parameters of both the converter and the switching modulation technique to limit the switching frequency to a certain value. Then, this minimum inductance is slightly increased to get a total inductance L_d that establishes a switching frequency margin to the upper-limit. Thus, the total inductance obtained proves to be physically smaller and thus, less expensive.

- *Resonance frequency of the filter*: The frequency bandwidth in active filters is wide (defined by various harmonic standards). They are principally different from those of grid-connected reactive compensators. In this design, however, the resonance frequency (f_{res}), as the nonzero poles of the admittance seen from the ac/dc converter (see (2)), depends on the highest frequency component of the load which is compensated by an active filter.
- *Minimization of stabilizing resistors*: The equivalent impedance of the passive *LCL*-filter approaches zero at the resonance frequency and it will consequently lower the stability margin of the system down. To avoid instability, a resistor R_d is used in series with the capacitor. The resistance R_d is normally selected in proportion to the capacitive reactance of the filter at the resonance frequency ($1/2\pi f_{res}C$) [3]. This resistance can be chosen such that it minimizes the power dissipation too.
- *Maximizing the attenuation at switching frequency*: Using Fig. 1(b), three transfer functions can be worked out that describe the passive filter behavior:

$$\begin{cases} Y_{12}(s) = \dfrac{i_1(s)}{v(s)} = \dfrac{(1/L_1)(s^2 + (1/L_2C))}{s(s^2 + (L_1 + L_2/L_1L_2C))} \\ Y_{21}(s) = \dfrac{i_2(s)}{v(s)} = \dfrac{(1/L_1L_2C)}{s(s^2 + (L_1 + L_2/L_1L_2C))} \\ h_{22}(s) = \dfrac{i_2(s)}{i_1(s)} = \dfrac{(1/L_2C)}{(s^2 + (1/L_2C))} \end{cases} \tag{2}$$

The required performance from the passive *LCL*-filter can be assessed under different conditions. For high frequencies (e.g. switching frequency f_{sw}), the admittance $Y_{12}(s)$ approaches $(1/L_q s)$. This shows the importance of choosing a proper value for the inductance L_1. Considering the IEC standard 61000-3-4 [1], the amplitudes of the currents above the 33rd harmonics have to be smaller than 0.6% of the fundamental harmonic. This can be applied to the passive filter to attenuate harmonic currents at the switching radian frequency ϖ_{sw}:

$$\left|Y_{21}(s = j\varpi_{sw})\right| \leq 0.006 \tag{3}$$

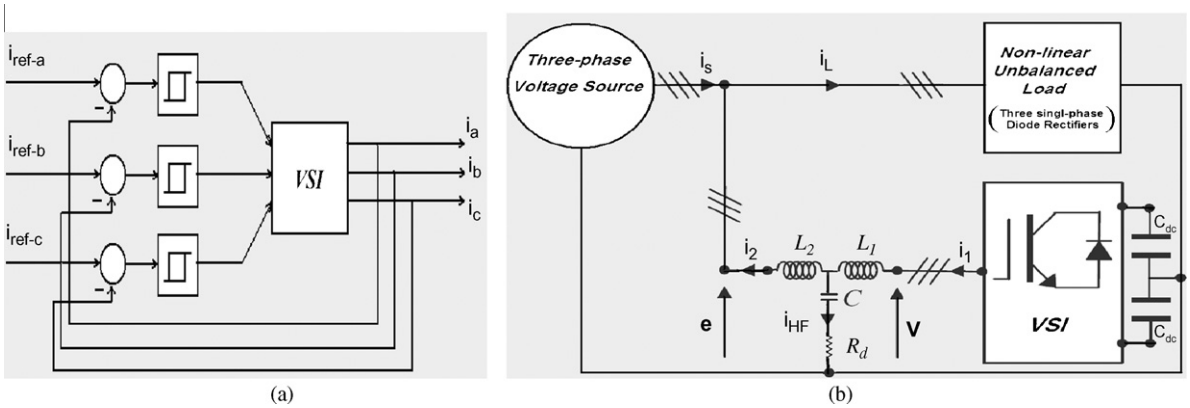

Fig. 1. (a) A typical current-control of a voltage-sourced inverter using the hysteresis modulation technique, (b) an active filter consists of an *LCL* passive filter that interconnects a VSI to the grid system.

It is also necessary to decrease both $|Y_{12}(s=j\varpi_{sw})|$ and $|h_{22}(s=j\varpi_{sw})|$ to the smallest possible value.

2.1. Inductance ratio

To design two inductances for the *LCL*-filter, the following precautions must be taken in order to develop a proper passive filter for the active filter.

- The admittance $|Y_{12}(s)|$ in (2) includes three poles (p) and two zeros (z), while zeros are related to the nonzero poles as follows:

$$z = \pm j\sqrt{\frac{1}{L_2C}}, \quad p = \pm j\sqrt{\frac{L_1+L_2}{L_1L_2C}}$$
$$p = k'z, \qquad k' = \sqrt{1+\frac{L_2}{L_1}} = \sqrt{1+k} \tag{4}$$

  It can be seen that when the inductance ratio ($k=(L_2/L_1)$) becomes bigger, then the *nonzero poles distance away from zeros*. This would increase the overshoot amplitude and thus influences the performance of the filter. On the other hand, lowering k will decrease the overshoot inversely and proportional to k'.
- Current ripples of the capacitive branch (i_{HF}) passes through the stabilizing resistor R_d, which will lead to power losses equal to $R_d i_{HF}^2$. While the dc/ac converter supplies the dissipated power on R_d, the dc voltage controller absorbs active power from the source in order to compensate the dc voltage drop. This will eventually cause an increase of the source current. Meanwhile, the low order harmonics should be highly attenuated by L_1, and the higher order of harmonics by L_2 and C. Since the magnitudes of high order harmonics are normally small, this will considerably lowers the power dissipation on R_d.
- Let us call the loop containing the switching converter, L_1 and the capacitive branch of the *LCL*-filter in Fig. 1(b) as the internal loop. When $L_2 > L_1$, then high frequency current oscillations increase through the internal loop. This increases the ratings of the switches and at the same time raises the cost and switching losses. To avoid over-current limitation, the designer can use parallel switches.
- The transfer function $h_{22}(s)$ in (2) suggests that choosing big values for L_2 provides higher attenuation for harmonics of the output current i_2 in comparison with the input current i_1. Thus, the relationship $L_2 > L_1$ (or $k > 1$) has already been appeared in literatures (e.g. [4]).
- Choosing the ratio k has no special effect on transfer function $Y_{21}(s)$ in (2).
- An *LCL*-filter comprises more energy storage elements than a passive *L*-filter, and this slows down the dynamic characteristics of the filter. Hence, switching frequencies are more limited for an *LCL*-filter with respect to a dynamically faster *L*-filter. Also, when an *LCL*-filter is designed using $k < 1 (L_2 > L_1)$, then the switching frequencies involved in current-controlled modulation become lower than those of $k < 1 (L_2 > L_1)$. This could be advantageous since very fast switches are not necessary, while it can also be argued that employing fast switches is, theoretically, advantageous.

Considering above points, choosing big values for L_2 lowers i_2 distortion; although this constitutes *higher cost* and *power losses* for the system compared to smaller L_2. Thus, the relationship $L_2 > L_1$ can be suggested to achieve *high efficiency* and to avoid possible *overrating* of the switches by choosing a low value for k.

2.2. Capacitance and resistance

The following points should be considered in order to decide on the values of the capacitance and resistance of the *LCL*-filter:

- Two transfer functions $Y_{12}(s)$ and $h_{22}(s)$ in (2) show that bigger values of capacitance C, will further attenuates the higher frequencies.
- It is suggested in [3] that the value of damping resistor R_d should be chosen proportional to the capacitive reactance at resonance frequency ($1/2\pi f_{res}C$).
- Moreover, it is necessary to design both i_{HF} and R_d as low as possible to avoid additional power losses imposed to the source by R_d.
- Transfer functions given by (2) are obtained when $R_d = 0$. Nevertheless, when nonzero values are selected for R_d, the poles will contain both real and imaginary parts. Imaginary parts of the poles are decreased toward zero by increasing R_d. Hence, choosing a big value for R_d could lead to a pure real pole, which acts as a pure attenuator for all frequencies. This would result in losing the filtering operation of the *LCL*-filter based on the frequency modulation.

3. Design procedure

Considering (1), the minimum value of the total inductance is derived for an inductive filter in order to limit the maximum switching frequency. Those active filters which use a hysteresis-like switching modulation have a variable switching frequency within $[f_{min}, f_{max}]$. Maximum switching frequency that is given for the hysteresis technique is as follows [8]:

$$f_{max} = \frac{V_{dc}}{8hL} \tag{5}$$

where V_{dc} is the dc-link voltage, h is the hysteresis-band (e.g. 5% of peak current) and L is the inductance of a first-order inductive filter. Using (5), the minimum required inductance is equal to $L_{min} = (V_{dc}/8hf_{max})$, which is a boundary value. Hence, to make sure f_{max} is properly limited, the total inductance L_d can be chosen as a multiple (bigger than one) of L_{min} as below:

$$L_d = \alpha L_{min} \tag{6}$$

Further, it is recommended in [4] that L_d should be smaller than 0.1 P.U. in order to limit the voltage drop on the total inductance. Thus, using (6) the upper-limit for α can be given by

$$\alpha \le \frac{0.1(\text{P.U.})}{L_{min}(\text{P.U.})} \tag{7}$$

3.1. Deciding on LCL parameters

Moreover, the resonance frequency f_{res} is suggested in [9] to be chosen within $[(5–10)f_s, (1/2)f_{sw}]$ for those static compensators that work mainly with synchronous frequency f_s. But this chosen lower-limit is not appropriate for active filters, due to the fact that it falls within the compensating bandwidth of active filters. The upper-limit of active filters depends on a variable switching frequency range within $f_{sw} \in [f_{min}, f_{max}]$, depending on the modulating hysteresis-band. Therefore, the decisive region for the resonance frequency of active filters can be suggested as below:

$$f_{res} \in \left[(1.2–1.3)f_{cmax}, \frac{1}{2}f_{min}\right] \tag{8}$$

where the frequency f_{cmax} represents the compensating bandwidth at the highest harmonic order of the load that is to be compensated by the active power filter. Then, using the nonzero poles of $Y_{12}(s)$ in

(2), the resonance frequency can be introduced in terms of k and C by (Appendix 1 details derivation of (9)):

$$f_{\text{res}} = \frac{1}{2\pi}\frac{1+k}{\sqrt{kL_{\text{d}}C}} \tag{9}$$

Relationships (8) and (9) impose further limitations on the selection of f_{res}, k and C.

As was discussed in Section 2.2, the capacitance C can be as large as possible. Also, for a certain C and a fixed L_{d}, the bigger the inductance ratio k, the lower the resonance frequency will be. (This can be shown mathematically because when $k \in [0, 1]$, derivative of (9) with respect to k will always be negative.) Therefore, a desired resonance frequency can be obtained by selecting an appropriate k with a large C. One can also apply (3) to both $Y_{12}(s)$ and $Y_{21}(s)$ introduced by (2).

3.2. The EMI noise suppression

Conductive EMI emitted by semiconductor switches is that of a pulse train as differential-mode noise, which consists of repetitive switch-on and switch-off transitions (including reverse recovery time of diodes). Moreover, the EMI of power electronics is qualified as broadband, paving the way for defining the spectrum of a single impulse instead of performing a discrete harmonic analysis of the pulse train [7]. In general, the EMI spectra of power semiconductor devices are below a few megahertz.

Thus, one can derive the *ABCD* parameters for Fig. 1(b), where the passive *LCL*-filter is connected to the converter from one end and to an equivalent power system bus from the other end. Also, assume the converter-end equivalent impedance is zero, and the power system is represented by an independent voltage source behind a series inductance L_{g}. Then, the *insertion loss* (IL) for the described filter combination can be simplified on the basis of the formula given in [7] as follows:

$$\begin{cases} \text{IL}(s) = 20\ \log\dfrac{A(s)\times L_{\text{g}}s - B(s) + C(s)\times L_{\text{g}}s\times 0 - D(s)\times 0}{L_{\text{g}}s + 0} \\ A(s) = 1 + L_1Cs^2, \quad B(s) = -s(L_1 + L_2Cs^2) \end{cases} \tag{10}$$

In above formula, the zeros represent the converter internal impedance. Replacing s with $j\omega$, and substituting $A(s)$ and $B(s)$ in |IL| will result in

$$\left|\text{IL}(s = j\omega)\right| = 10\log\left[\left(1 - \frac{L_1}{L_{\text{g}}} - L_1C\omega^2\right)^2 + \left(\frac{L_2}{L_{\text{g}}}C\omega\right)^2\right] \tag{11}$$

For the frequencies in the conductive EMI disturbance mode (above 150 kHz), the given |IL| in (11) can be well approximated by

$$\text{IL}(s = j\omega)| \approx 20\ \log(L_1C\omega^2) \tag{12}$$

This clearly describes the effect of L_1 on the IL. The bigger the inductance L_1 and the capacitance C, the bigger will the resultant |IL| be that is produced by the passive *LCL*-filter. This is to say that more attenuation will result in the spectra of the EMI conductive noise, which is in line with the foregoing conclusions on choosing larger capacitance C and larger L_1 under $k < 1$ constraint.

3.3. Summarized design procedure

In brief, the design algorithm of the passive *LCL*-filter can be described as follows:

1. Consider a switching frequency region that is based on the defined active filter bandwidth f_{cmax}, the modulation technique, and the technical limitation of the employed switches, i.e. $f_{\text{sw}} \in [f_{\text{min}}, f_{\text{max}}]$.
2. Choose a compensating algorithm (e.g. like (14)) with which the active filter would be able to satisfy pre-determined objectives. Simulate the chosen algorithm to find the minimum peak-to-peak current of the active filter amongst the three phases. A small fraction of this current (e.g. 5%) can be used as the hysteresis-band h. Then, calculate L_{min} and L_{d} using (5)–(7) by selecting a suitable α.
3. Calculate the region of resonance frequency using (8), and plot f_{res} in (9) versus different values for k and C. Select the biggest possible value for C that gives the lowest possible resonance frequency. Then, find a feasible region for k using the following simplified equation obtained from combining (8) and (9):

$$\begin{cases} k^2 - (m^2 - 2)k + 1 = 0 \\ m = 2\pi f_{\text{res-b}}\sqrt{L_{\text{d}}C} \end{cases} \tag{13}$$

   where the frequency $f_{\text{res-b}}$ is replaced with either boundary of f_{res}. This will lead to determination of the upper and lower limits for k. Choose a value for k close to the calculated upper-limit, and hence determine L_1, L_2 and f_{res}.
4. Evaluate three transfer functions $Y_{12}(s)$, $Y_{21}(s)$ and $h_{22}(s)$ introduced in (2) at the switching frequency using the parameters obtained in the previous steps. If the standard expressed by (3) holds for both $Y_{12}(s)$ and $Y_{21}(s)$, then the design of the *LCL*-filter will be done with. Otherwise, the design procedure has to be continued on using the third step by changing the design parameters C and k.

4. Designing an *LCL*-filter for a typical power system

Assume the three-phase 50 Hz power system of Fig. 1(b) with three symmetrical voltages of 200 V (RMS). Also, assume that an asymmetrical three-phase load of 16 kVA is connected to the supply, consisting of three single-phase diode rectifiers. Fig. 2 shows the load currents. It is intended to employ an active power filter. Inclusion of the active filter is to compensate for the load harmonics (initial conditions of all inductances at $t = 0$ are equal to zero). The bigger the ratio of dc-link voltage of the active filter over the magnitude of load-terminal voltage (converter gain), the larger will be the total inductance connecting the converter to the network. While this gain is suggested to be 1.05 in [10], it is proposed to be raised up to 2 in [11,12]. Let us assume this gain to be about 1.53 for this design, yielding a dc voltage of $V_{\text{dc}} = 1.53 \times \sqrt{2} \times \sqrt{3} \times 200 \cong 750$ V. An optimized solution is introduced in [13], which is used in this paper in order to generate three-phase current references for the active filter $\mathbf{i}_{\text{C-ref}}$ as follows:

$$\boldsymbol{i}_{\text{C-ref}}(t) = \boldsymbol{i}(t) - \frac{\overline{P(t)}}{v(t)\cdot v(t)}v(t) \tag{14}$$

where $\mathbf{i}(t)$ contains the three-phase load currents, $\mathbf{v}(t)$ includes the three-phase load-terminal voltages, $\overline{P(t)}$ is the average active power consumed by the load and the dot product $\mathbf{v}(t)\cdot\mathbf{v}(t)$ represents the

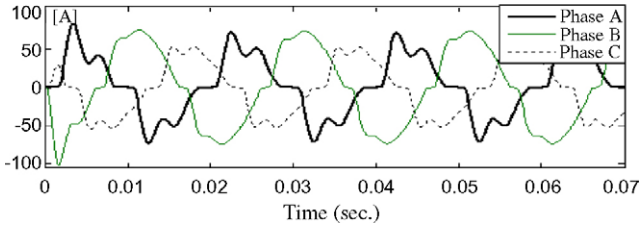

Fig. 2. Waveforms of the three-phase load currents.

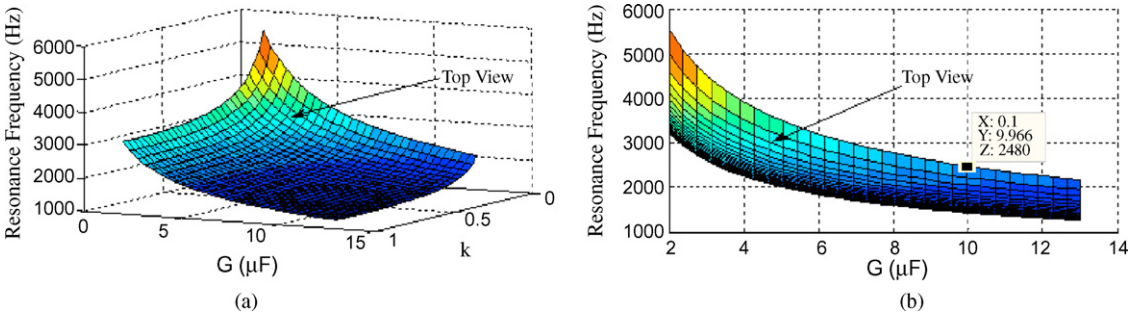

Fig. 3. Variations of resonance frequency drawn versus the inductance ratio k along with the capacitance C, (a) three-dimensional view, and (b) two dimensional view f_{res} against C.

well-known definition of instantaneous active power of the load [13]. The second-term in the right hand side of (14) is the desirable optimal source current that is subtracted from the load current in order to achieve the required compensating reference current (Appendix 1 details derivation of (14)).

4.1. Total inductance L_d

Further, assume the exact currents of the active filter trace that the optimized references introduced by (14) using a hysteresis current-control strategy. In practice, employing IGBT power switches would limit the maximum *practical* switching frequency. Let us choose the maximum modulation frequency $f_{max} = 9$ kHz, and the region for the modulation switching frequency as $f_{sw} \in [6, 9]$ kHz. The compensating rule of (14) was simulated with SIMULINK. Simulations show that the minimum peak-to-peak current of the active filter is equal to 60 A, belonging to phase b. Also, assume the peak-to-peak of the ripples equals 10% times 60 A, resulting in a hysteresis-band of $h = 3$ A. Hence, the minimum required inductance can be calculated by using (5) as below:

$$L_{min} = \frac{V_{dc}}{8hf_{max}} = \frac{750}{8 \times 3 \times 9} = 3.47\ \text{mH} \tag{15}$$

Choosing $\alpha = 1.3$ will result in $L_d = 4.5$ mH, according to (6). It is noticeable that the maximum switching frequency is now limited to about 6.95 kHz for the hysteresis modulating strategy using (5). Also, f_{res} is affected by the chosen k and C based on (9), which is described by the following subsection.

4.2. Resonance frequency f_{res}, inductance ratio k and capacitance C

Assume the highest harmonic order for the compensation is the 40th (i.e. $f_{cmax} = 40 \times 50 = 2$ kHz). Considering (8), applying a factor 1.25 to f_{cmax} results in a lower limit of 2.5 kHz along with an upper-limit of 3 kHz ($0.5 \times f_{min} = 3$ kHz) for the resonance frequency. Also, if the total inductance $L_d = 4.5$ mH is replaced in (9), then f_{res} along with k and C are subjected to the following constraints:

$$\begin{cases} 2500 \le f_{res} \le 3000 \\ f_{res} = \dfrac{1}{2\pi} \dfrac{(k+1)}{\sqrt{0.0045}\sqrt{kC}} = 2.37 \dfrac{(k+1)}{\sqrt{kC}} \end{cases} \tag{16}$$

There are three unknown parameters in (16), while both available relationships are depicted in Fig. 3(a) and (b). Combining these two relations will lead to a feasible region for k and C. Using the described design procedure, a big C should be selected with a small k in the feasible region which would give the desired resonance frequency. Hence, a feasibly big capacitance can be chosen like $C = 10$ μF using Fig. 3. Then, satisfying the resonance frequency region would lead to a feasible region for the inductance ratio $k \in [0.0718, 0.1110]$ using (13). Therefore, a value for k is chosen close to 0.1110 from this region, i.e. $k = 0.1$, resulting in $f_{res} = 2607$ Hz, $L_1 = 4.1$ mH and $L_2 = 0.4$ mH.

4.3. Transfer functions

It is necessary for the transfer functions $Y_{12}(s)$ and $Y_{21}(s)$, described by (2), to satisfy the IEC standard 61000-3-4 [1] shown by (3) for the switching frequency region ([6000, 9000] Hz). Fig. 4(a)

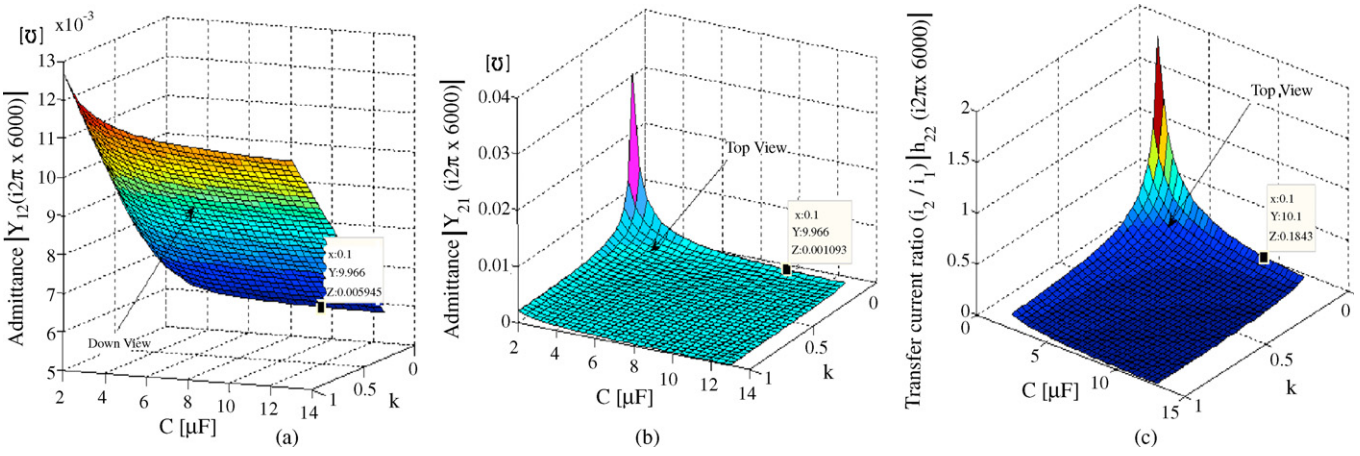

Fig. 4. Magnitudes of the three transfer functions described by (2) at the lowest switching frequency 6 kHz against the variations in the inductance ratio k and the capacitance C, (a) the admittance $|Y_{12}(j2\pi \times 6000)|$, (b) the admittance $|Y_{21}(j2\pi \times 6000)|$, and (c) the transfer current ratio $|h_{22}(j2\pi \times 6000)|$.

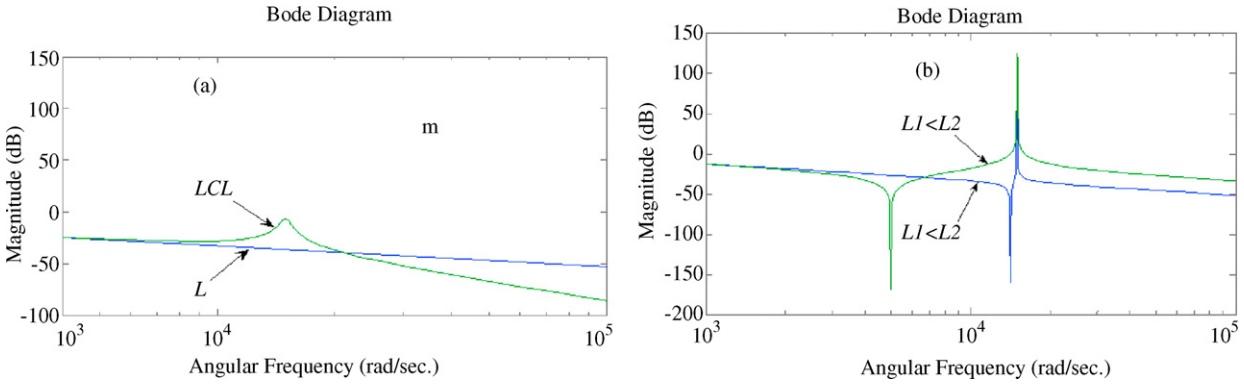

Fig. 5. Bode diagrams related to magnitudes of low-pass passive filters, (a) *L*-filter compared to *LCL*-filter, and (b) two *LCL*-filters (the case $L_1 > L_2$ compared to the case $L_1 < L_2$).

Table 1
Summarized list of parameters related to the designed passive *LCL*-filter that is used as an active power filter for a power system

Supply phase voltage	200 Vrms
Grid frequency	50 Hz
Source inductance	0.1 mH
APF side *LCL*-filter inductance, L_1	4.1 mH
Grid side *LCL*-filter inductance, L_2	0.4 mH
LCL-filter capacitor, *C*	10 μF
LCL-filter damping resistor, R_d	20 Ω
APF switching frequency	[6, 9] kHz
APF dc-link capacitors (each one)	2 mF
APF dc-link voltage, V_{dc}	750 V

illustrates the magnitude of the admittance $Y_{12}(s)$ for various values of k and C, when the switching frequency is fixed at 6 kHz (modulating frequencies higher than 6 kHz give lower magnitudes). It can be seen that for the selected values of k and C (0.1 and 10 μF) the magnitude of this admittance satisfies (3) ($|Y_{12}(j2\pi \times 6000)|$=0.005945). Similarly, the transfer function $Y_{21}(s)$ is shown by Fig. 4(b). Magnitude of $Y_{21}(s)$ is also in agreement with (3) at 6 kHz ($|Y_{21}(j2\pi \times 6000)| = 0.001093$).

Furthermore, Fig. 4(c) shows $|h_{22}(s)|$ at 6 kHz versus k and C. For the selected values of k and C, the output current i_2 is attenuated by about five and a half times with respect to the input current i_1 ($|h_{22}(j2\pi \times 6000)| = 0.1843$).This suggests that high frequency components are considerably attenuated despite choosing $L_1 > L_2$. But this has the advantage of lower oscillations with high magnitudes at the converter-side of the *LCL*-filter (i.e. this improves the efficiency (see Section 2.1)). Designed parameters of the above *LCL*-filter satisfy all the discussed objectives. Meanwhile, for a certain *LCL*-design, if one or more chosen parameters disagree with the objectives, then different values for k and C are used to make a new design. This may be continued on until the desired design is obtained.

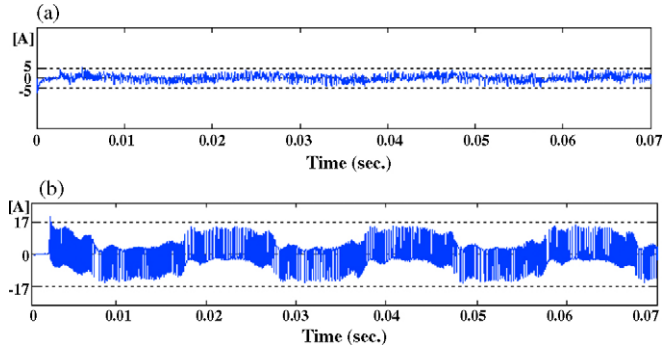

Fig. 7. Comparison of the remained high frequency components of the active filter flown into the *LC*-section of the *LCL*-filter for two cases, (a) when $L_1 > L_2$, and (b) when $L_1 < L_2$.

4.4. Comparison of the designed LCL-filter with equivalent L-filter

Let us compare the above designed *LCL*-filter with an *L*-filter in which the total inductances in both passive filters are identical. The attenuating resistance of the *LCL*-filter is assumed to be $R_d = 3 \times (1/2\pi f_{ref} C) \approx 20\ \Omega$. Hence, the Bode diagrams of both passive filters are depicted in Fig. 5(a). Both diagrams introduce similar behavior for frequencies less than f_{res} that will meet the design objectives. Moreover, the *LCL*-filter shows bigger attenuations than those of the *L*-filter for frequencies greater than f_{res}. Table 1 summarizes all the designed parameters including the parameters of both the active power filter and the power system.

5. Simulations and discussions

Consider the power system in Fig. 1(b) that comprises a three-phase power source supplying the three-phase currents shown by

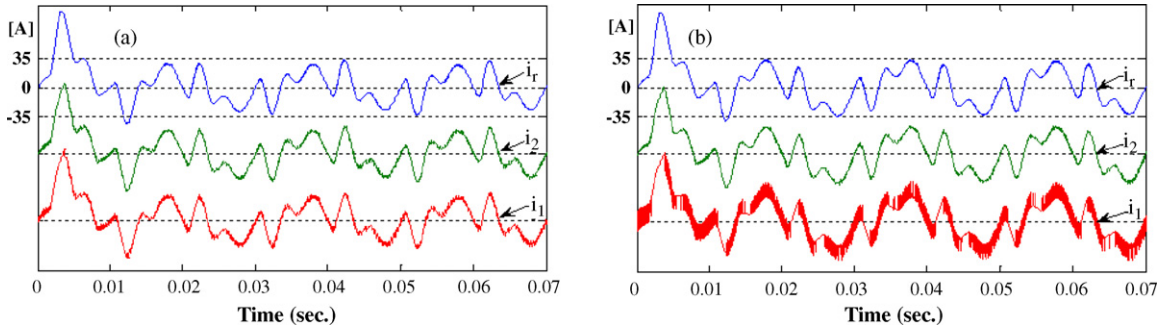

Fig. 6. Reference current of the active filter i_r along with the input current i_1 and output current i_2 of the *LCL*-filter at phase a, (a) when $L_1 > L_2$, and (b) when $L_1 < L_2$.

Table 2
Comparison of the designed *LCL*-filter performance with an extreme case where inductances are swapped

	The RMS current through R_d (A)	Three-phase power losses dissipated by R_d (W)
Case 1 ($L_1 > L_2$)	1.6	170
Case 2 ($L_1 < L_2$)	5.6	2100

Fig. 2 to a non-linear load. An active filter is also connected across the load terminal to compensate load harmonics. The designed *LCL*-filter in Section 3 is used as its passive filter. This power system is simulated with SIMULINK to investigate the suitability of the proposed passive *LCL*-filter. Designed *LCL*-filter is utilized for two sets of parameters, the first being in accordance with the proposed method ($k = 0.1, L_1 > L_2$), while the second will be in accordance with an extreme condition in which the two inductances are swapped ($k = 10$, $L_1 < L_2$). These two cases are examined not only to justify the suggested design of the first case, but also to show the consequences of an ill-conceived *LCL*-filter on the performance of the whole active filter (e.g. the efficiency and EMI issues). Both cases are simulated and comparative discussions are presented.

5.1. Bode diagrams

Bode diagrams of the two cases are depicted in Fig. 5(b) in which R_d is equal to zero. When $L_1 > L_2$, nonzero poles are closer to the zeros of the *LCL*-filter compared to those of the case $L_1 < L_2$, resulting in smaller undesirable region for the filter. Additionally, better attenuation at higher frequencies will result for the case when $L_1 > L_2$ is compared to $L_1 < L_2$ case.

5.2. Simulation results

Reference currents are initially obtained using (14) for the active filter. Then, these references are traced by the exact currents of the active filter using a hysteresis current-control modulation technique. Simulations are introduced in Fig. 6(a) and (b) for both cases $L_1 > L_2$ and $L_1 < L_2$, respectively. Each picture includes reference current for phase a of the active filter i_r, the internal current i_1 and external current i_2 of the *LCL*-filter. It is noticeable that both cases have identical references in which the RMS and maximum peak of the reference currents are 18 and 32 A, respectively. Also, the references are compared with the external currents i_2 for the hysteresis pulse width modulator.

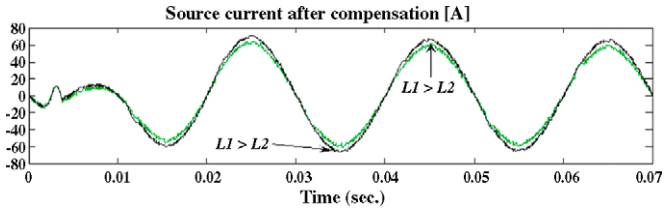

Fig. 8. Comparison of the source current after compensation for two cases, $L_1 > L_2$, and $L_1 < L_2$.

It can be seen from Fig. 6(a) that the case $L_1 > L_2$ nearly cancels frequency components available in i_1 related to the switching frequency. Only *a small part of high frequency components* flows into the remaining L_2C-section of the passive *LCL*-filter. On the other hand, Fig. 6(b) shows that the case $L_1 < L_2$ includes considerable ripples on top of i_1, rushing *significant high frequency components* as well as *considerable low order harmonics* into the remaining L_2C-section.

5.2.1. Efficiency and rating of switches

Frequency components that flow into the L_2C-section of the *LCL*-filter impose additional power losses to the active filter. This clearly lowers the efficiency of the filter, which is problematic in higher power levels. Fig. 7(a) introduces the high frequency components flowing into the capacitive branch when $L_1 > L_2$. This current passes through the resistance R_d (1.6 A, RMS), leading to three-phase power losses about 170 W. This can be compared with the case $L_1 < L_2$ which is illustrated in Fig. 7(b). Here, the RMS current through R_d is equal to 5.6 A, resulting in three-phase power losses of about 2100 W.

Table 2 summarizes the calculated RMS current flowing into capacitive branch together with the resultant three-phase power losses for both cases. While the RMS current of the first case ($L_1 > L_2$) is 3.5 times lower than that of the second case ($L_1 < L_2$), the resultant three-phase power losses of the second case is 12.35 times bigger than that of the first case. Thus, an ill-conceived *LCL*-filter design is subjected to both low and high frequency components and power losses bigger than those of the proposed method in the first case.

Moreover, the source current i_S after compensation is presented by Fig. 8 for both cases. While the RMS current of the source is equal to 38.9 A for the first case, the calculated RMS source current equals 46.8 A for the second case. This shows the RMS difference between the two cases to be about 7.9 A, lowering the RMS value about 17%. These pictures also show that the first case represents lower peak current about 11 A compared to the second case.

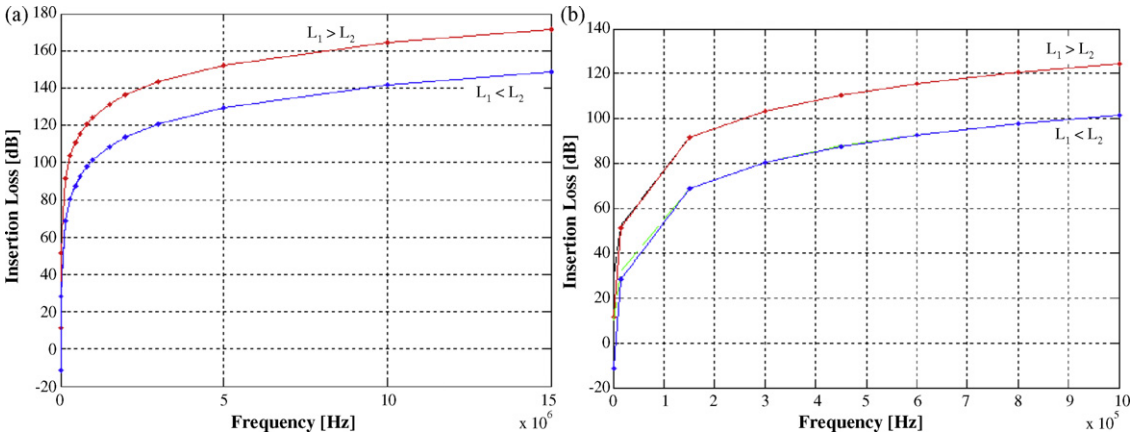

Fig. 9. Insertion loss of the *LCL*-filter (showing the level of attenuation) at different frequencies for the two studied cases, (a) zooming out the frequencies up to 15 MHz, and (b) zooming in the frequencies up to 1 MHz.

Table 3
Comparison of the calculated |IL| for the two cases up to 15 MHz to show the significant attenuating performance of the first case over the second one

	kHz													
	1.5	15	150	300	450	600	800	1000	1500	2000	3000	5000	10,000	15,000
dB														
IL ($L_1 > L_2$)	30.3	52.06	91.44	103.48	110.52	115.52	120.52	124.39	131.43	136.43	143.48	152.35	164.39	171.43
IL ($L_1 < L_2$)	9.99	31.96	68.56	80.56	87.60	92.60	97.60	101.47	108.51	113.51	120.55	129.43	141.47	148.51

Furthermore, the peak current flowing through the switches of the active filter is 34 A in the first case and 55 A in the second case. This clearly shows the influence of a well-designed *LCL*-filter on the current ratings of the switches compared to the second case as an extreme situation. It is noticeable that both cases provide almost *identical THD* of about 2.8%.

5.2.2. The EMI issue

The IL of the *LCL*-filter is introduced by (11), and approximated by (12). Both relationships have been simulated with MATLAB for frequencies up to 15 MHz. Since the spectra of the EMI of the switching semiconductors are below a few MHz, the simulated frequency range covers the behavior of the *LCL*-filters under the EMI conductive noise. Fig. 9(a) shows the |IL| in dB for frequencies within [0, 15] MHz. It can be seen that when $L_1 > L_2$ (the first case) the |IL| is bigger than that of the second case $L_1 < L_2$. Fig. 9(b) zooms at the frequency range of [0, 1] MHz in order to show the advantage of the first case in the EMI spectra starting from 150 kHz over the second case. This presents a significant attenuation difference between the two cases for high frequencies, confirming the first case as the superior one. Moreover, both (11) and (12) (exact and approximated |IL|) are shown in Fig. 9(a) and (b) for the two cases and are identical. Table 3 compares the calculated |IL| for the two cases for 14 different frequencies to emphasize on the discussed points.

5.2.3. Practical validation

The second case is typically implemented in [4], which introduces practical results in agreement with the simulations related to the second case. Also, recently a power electronic modeling of active filters is presented in [14], which uses an *LCL*-filter with parameters that are obtained using the suggested procedure like those of the first case (Ref. [14] provides *no* description on how the *LCL*-filter parameters are designed). Simulations of the first case agree with the practical results in [14].

6. Conclusion

An *LCL* passive filter is often employed for an active filter instead of a simple *L*-filter in order to achieve significant benefits. Since active filters are designed to compensate harmonics up to a predetermined orders by different standards (e.g. IEEE 519-1992), flow of these frequency components through the *LCL*-filter is highly sensitive to its designed parameters. Moreover, the EMI conductive noise caused by switch-on and switch-off as well as the reverse recovery of diodes could be treated properly if the passive *LCL*-filter is well-designed. Further, the sensitivity of the *LCL*-filter to the designed parameters would be accentuated if a fixed-band hysteresis modulation technique is used. This paper proposes a procedure of designing a passive *LCL*-filter to be applied to active filter applications. First, various points and characteristics are described related to the constituent inductances, capacitance and damping resistance. A design procedure is then presented, which is applied to a typical active-filtering application. Then, using the designed parameters, the active power filter is simulated with SIMULINK to verify the proposed design method. Simulations indicate that the designed parameters of the *LCL*-filter affect the improvement of the efficiency of the active filter considerably and lower the ratings of the power switches. It also analyzes the effect of a well-designed passive *LCL*-filter on increasing its insertion loss in the range of the EMI conductive radio frequencies. This has been programmed with MATLAB, showing significant increase of more than 20 dB in the insertion loss of the well-designed *LCL*-filter.

Appendix A. Derivation of (9) and (14)

- Derivation of (9): Eq. (9) can be derived using the nonzero poles of (2) that is expressed in (4) like

$$f_{res} = \frac{1}{2\pi}\sqrt{\frac{L_1+L_2}{L_1L_2C}} = \frac{1}{2\pi}\sqrt{\frac{1+(L_2/L_1)}{L_2C}} \tag{1-1}$$

Multiplying both numerator and denominator of (1-1) by $\sqrt{1+(L_2/L_1)}$ results in

$$f_{res} = \frac{1}{2\pi}\sqrt{\frac{(1+(L_2/L_1))^2}{(1+(L_2/L_1))L_2C}} = \frac{1}{2\pi}\sqrt{\frac{(1+(L_2/L_1))^2}{(L_1+L_2)(L_2/L_1)C}} \tag{1-2}$$

Substitution of (L_1+L_2) with L_d, and $L_2 > L_1$ with k, defined by (1), finally gives (9) as follows:

$$f_{res} = \frac{1}{2\pi}\sqrt{\frac{(1+k)^2}{L_dkC}} = \frac{1}{2\pi}\frac{1+k}{\sqrt{L_dkC}} \tag{1-3}$$

- Derivation of (14): The following optimization problem minimizes the active power supplied by the source:

$$\begin{cases} \text{minimize} & (i_a(t)-i_{qa}(t))^2+(i_b(t)-i_{qb}(t))^2+(i_c(t)-i_{qc}(t))^2 \\ \text{Subjected to} & v_a(t)i_{qa}(t)+v_b(t)i_{qb}(t)+v_c(t)i_{qc}(t)=0 \end{cases} \tag{1-4}$$

where (v_a, v_b and v_c) and (i_a, i_b and i_c) represent the load voltages and currents, respectively and (i_{qa}, i_{qb} and i_{qc}) show the reactive part of the load currents that their contribution in generating active power is zero (shown by the constraint). Solving this combinatorial problem using the Lagrange method gives the solution given by (14).

Appendix B. List of mathematical symbols

ABCD	the ABCD parameters of the *LCL*-filter
C	the capacitance of the *LCL*-filter
f_{cmax}	the highest harmonic of the load
f_{max}	maximum frequency of the modulator
f_{min}	minimum frequency of the modulator
f_{res}	the resonance frequency
$f_{res\text{-}b}$	the boundary resonance frequency
f_s	the synchronous frequency
f_{sw}	the switching frequency
h	hysteresis-band
h_{22}	currents transfer ratio
i_1	the current through L_1
i_2	the current through L_2

i_{HF}	current ripples of the capacitive branch
IL	insertion loss
k	the ratio of inductances of the *LCL*-filter
L_1	the converter-end inductance of the *LCL*-filter
L_2	the network-end inductance of the *LCL*-filter
L_d	the total inductance of the passive *LCL*-filter
L_g	the source inductance
L_{min}	minimum required total inductance
p	pole
R_d	damping resistor
v	the converter voltage
V_{dc}	dc-link voltage of the APF
Y_{12}	admittance seen from the converter
Y_{21}	admittance transfer ratio related to i_2
z	zero

References

[1] M. Bojrup, Advanced control of active filters in a battery charger application, Ph.D. Thesis, Lund Institute of Technology, Lund, Sweden, 1999.
[2] M. Lindgren, J. Svensson, Control of a voltage source converter connected to the grid through an LCL-filter—application to active filtering, in: Proceedings of the IEEE PESC'98, vol. 1, 1998, pp. 229–235.
[3] E. Twining, D.G. Holmes, Grid current regulation of a three-phase voltage source inverter with an LCL input filter, in: Proceedings of the IEEE PESC'02, vol. 3, 2002, pp. 1189–1194.
[4] M. Liserre, F. Blaabjerg, S. Hansen, Design and control of an LCL-filter-based three-phase active rectifiers, IEEE Transactions on Industry Applications 41 (2005) 1281–1291.
[5] Y. Lang, D. Xu, H.S. Handranamrei, H. Ma, A novel design method of LCL type utility interface for three-phase voltage source rectifier, in: Proceedings of the IEEE PESC'05, vol. 1, 2005, pp. 313–317.
[6] H.R. Karshenas, H. Saghafi, Basic criteria in designing LCL filters for grid connected converters, in: Proceedings of the IEEE ISIE'06, vol. 1, 2006, pp. 9–12.
[7] L. Tihany, Electromagnetic Compatibility in Power Electronics, IEEE Press, 1995.
[8] B.K. Bose, An adaptive hysteresis-band current control technique of a voltage-fed PWM inverter for machine drive system, IEEE Transactions on Industrial Electronics 37 (1990) 402–408.
[9] F.H. Abdul-Magueed, On Power Electronics Interface for Distributed Generation Applications and its Impact on System Reliability to Customers, Chalmers University of Technology, Goteborg, Sweden, 2005.
[10] S. Kwak, H. Toliyat, Design rating comparisons of PWM voltage source rectifiers and active power filters for AC drives with unity power factor, IEEE Transactions on Power Electronics 20 (2005) 1133–1142.
[11] B.N. Singh, P. Rastgoufard, B. Singh, A. Chandra, K. Al-Haddad, Design, simulation and implementation of three-pole/four-pole topologies for active filters, in: Proceedings of the IEE-Electric Power Applications, vol. 151, 2004, pp. 467–476.
[12] M.K. Mishra, K. Karthikeyan, A study on design and dynamics of voltage source inverter in current control mode to compensate unbalanced and non-linear loads, in: Proceedings of the International Conference on PEDES'06, vol. 1, 2006, pp. 12–15.
[13] S. Fryze, Effective wattles and apparent power in electrical circuits for the case of non sinusoidal waveform of current and voltage, Elektrotechnische Zeitschr 53 (1932) 596–599.
[14] M. Tavakoli Bina, K.S. Ashoka, Bhat, Averaging technique for the modeling of STATCOM and active filters, IEEE Transactions on Power Electronics 23 (2008) 723–734.